Journal of Alloys and Compounds 480 (2009) 462–468

Contents lists available at ScienceDirect

Journal of Alloys and Compounds

journal homepage: www.elsevier.com/locate/jallcom

Thermal vacancy formation in Co-based Heusler-type alloys Co_2MnZ (Z = Si, Ge, Sn)

M. Kogachi [a], S. Kikuchi [a,1], T. Fujiwara [a,2], F. Hori [b,*]

[a] Department of Physical Science, Graduate School of Science, Osaka Prefecture University, Sakai, 599-8531, Japan
[b] Department of Materials Science, Graduate School of Technology, Osaka Prefecture University, Sakai, 599-8531, Japan

ARTICLE INFO

Article history:
Received 24 October 2008
Received in revised form 21 January 2009
Accepted 22 January 2009
Available online 6 February 2009

Keywords:
Intermetallics
Point defects
Vacancy formation
Positron spectroscopies

ABSTRACT

Thermal vacancy formation was studied for the Heusler-type ferromagnetic alloys Co_2MnZ (Z = Si, Ge, Sn) as a function of temperature (773–1273 K) by the density, electrical resistivity and positron annihilation measurements. The vacancy concentration increased with increase in quenching temperature and particularly, a high vacancy concentration exceeding 2% was observed in Co_2MnGe and Co_2MnSn. Estimated vacancy formation and migration energies were comparable with those for B2-type FeAl and CoGa alloys with high vacancy concentration. Further, the vacancy type and the vacancy site were examined for alloys quenched from 773 K. As a result, it was suggested that the mono-vacancies are randomly distributed over the lattice sites.

1. Introduction

Co-based Heusler-type ferromagnetic alloys Co_2YZ (e.g., Y = Cr and Mn and Z = Si, Ge, Sn and Al) are prospective candidates for application in the spin electronics devices because these are theoretically predicted to be half-metal ferromagnets with 100% spin polarization due to a gap at the Fermi level in the minority-spin band [1–3]. Despite the theoretical prediction, it is difficult to demonstrate the half-metallicity for these compounds. Some factors such as atomic disorder, nonstoichiometry and oxidation in the bulk and interface are thought to lead to degradation of the half-metallicity [2–4]. The Heusler ($L2_1$)-type structure with a chemical formula of X_2YZ consists of four fcc sublattices (symmetry group Fm3m), but as shown in Fig. 1, it can be also regarded as the structure consisting of eight bcc unit cells in which eight cube corner positions, X-sites, are occupied by X atoms, while eight body-centered positions are occupied alternately by Y atoms (Y-site) and Z atoms (Z-site). Atomic disorder occurs by deviating the composition from the stoichiometry or by elevating temperature from 0 K. Effect of this atomic disorder on the magnetic properties as well as the half-metallicity in the Co-based Heusler alloys Co_2YZ (X = Co) was recently examined from theoretical viewpoint [4–7].

A degree of atomic disorder can be well controlled by quenching from appropriate temperatures, because it varies depending on temperature. Recently, we have studied a relation between the atomic disorder and the magnetism for B2- and Heusler-phase $CoFe_{1-x}Al_x$ alloys [8,9] quenched from various temperatures. As a result, it was shown that atomic disorder on the Co-site, Co-type disorder, leads to degradation of the magnetism in the B2-phase, while the Fe–Al-type disorder (disorder between the Fe- and Al-sites) affects hardly the magnetism in the Heusler-phase. More recently, the same problem was studied for Heusler alloys Co_2MnZ (Z = Si, Ge and Sn) by our group [10], where the Co-type and Mn-Z-type defect concentrations have been determined by X-ray integrated intensity measurement for many reflections. It was found that both the defect concentrations increase with increase in quenching temperature in Co_2MnSi and Co_2MnGe, whereas in Co_2MnSn, only the Mn–Sn-type disorder proceeds. A relation between the atomic disorder and the mean magnetic moment observed in these alloys was also examined and it was concluded that the Co-type disorder leads to degradation of the magnetism, while the Mn–Z-type disorder affects hardly the magnetism. In this work [10], however, one problem remained to be solved, namely, about the change in lattice constant, a, with quenching temperature, T_Q. Fig. 2 shows the results for these alloys. The lattice constant a decreases with increase in T_Q up to 1073 K in Co_2MnSi and Co_2MnGe, rather slowly in the former and steeply in the latter, while in Co_2MnSn, it shows a steep decrease up to 1273 K. Further, an anomalous change in a occurs in Co_2MnSi and Co_2MnGe, i.e., the curves show an inflection above 1073 K. The authors [10] concluded that such behaviors cannot be systematically understood

* Corresponding author. Tel.: +81 72 254 9812; fax: +81 72 254 9812.
E-mail address: horif@mtr.osakafu-u.ac.jp (F. Hori).
[1] Kyocera Corporation, LTD, Shiga, 527-8555, Japan.
[2] NTN Corporation, LTD, Osaka, 550-0003, Japan.

0925-8388/$ – see front matter © 2009 Elsevier B.V. All rights reserved.
doi:10.1016/j.jallcom.2009.01.101

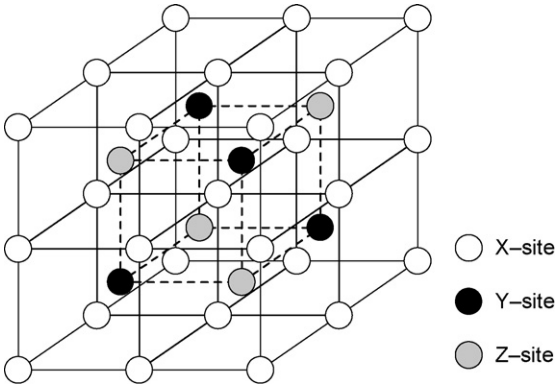

Fig. 1. Heusler ($L2_1$)-type X_2YZ ordered structure.

through a relation to the magnetic behavior, unlike the cases of B2-phase $Co_{1-x}Fe_x$ and $CoFe_{1-x}Al_x$ alloys [8,11], and then, they [10] suggested a possibility of formation of large amount of thermal vacancies.

Other than the antisite atoms that cause an atomic disorder mentioned above, vacancies are one of the major point defects. It is well recognized that some B2-type and $D0_3$-type binary alloys, XY (e.g., NiAl, CoGa and FeAl) and X_3Y (Fe_3Si and Fe_3Al), form a comparatively large amount of vacancies by deviating a composition from the stoichiometry or by elevating temperature [e.g., 12–18]. In particular, B2-phase $Fe_{1-x}Al_x$ alloys are known to retain easily a high concentration of thermal vacancies by quenching from high temperatures [15]. Then, the lattice constant shows a certain decrease with increase in quenching temperature, accompanying an increase in the retained vacancy concentration. The Heusler ($L2_1$)-type structure is thought to belong to the same family of bcc-based structures as the B2- and $D0_3$-type structures (as seen from Fig. 1, $L2_1$ is reduced to B2 when taking the atoms as Y = Z, and to $D0_3$ when X = Z, in binary alloy case). Thus, a possibility of formation of large amount of thermal vacancies can be reasonably expected. Such a situation has not been yet recognized experimentally for the Heusler-type alloys to date within the authors' knowledge. These basic structural data will give meaningful information for understanding the various physical and mechanical properties. In the present paper, we investigate the formation of thermal vacancies as a function of temperature (quenching temperature) for the Heusler Co_2MnZ (Z = Si, Ge and Sn) alloys. The density measurement is employed for determination of the vacancy concentration. The electrical resistivity and the positron annihilation measurements that are the excellent method for studying vacancy behaviors are also employed. The former is for estimation of vacancy migration, while the latter for examination of the vacancy type and the vacancy site.

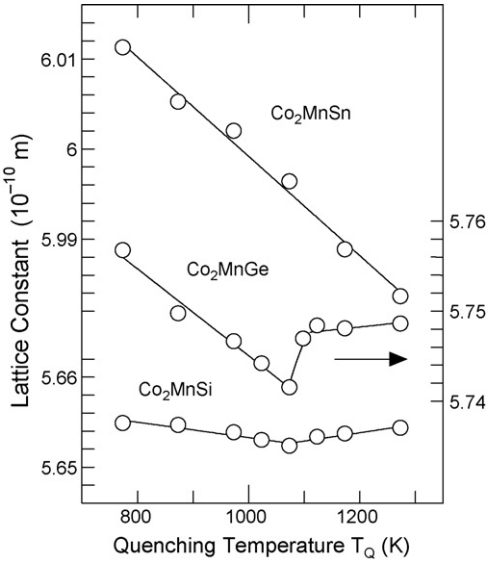

Fig. 2. Quenching temperature dependence of the lattice constant a in Co_2MnSi, Co_2MnGe and Co_2MnSn alloys. These data are quoted from Ref. [10].

2. Experimental procedures

Co_2MnZ (Z = Si, Ge and Sn) alloys were prepared by arc melting Co and Mn (purity of 99.99%) and Si, Ge and Sn (99.999%). Weight losses were less than 0.5%. Each ingot was homogenized at 1273 K for 50 h in a sealed silica tube filled with argon. The plate samples with a size of about 10 mm × 5 mm × 1 mm were prepared for density measurement. They were annealed at 1173 K for 2 h in silica tubes filled with argon, followed by cooling to room temperature at a rate of 2 K/min. Individual samples were again annealed at various temperatures from 773 K to 1273 K and then water-quenched (in quenching from temperatures above 973 K, the silica tubes were immediately crushed in water). Quenching temperature T_Q and holding time are, 773 K (25–50 d), 873 K (14–21 d), 973 K (5–7 d), 1073 K (24 h), 1173 K (5 h) and 1273 K (1 h). The density measurement was performed based on the Archimedes method using distilled water in the same way as described in [8,13–16]. The vacancy concentration, c_V, can be obtained from [13]

$$c_V = \frac{N_V}{N + N_V} = \frac{d_X - d_{obs}}{d_X} \quad (1)$$

where N and N_V represent the total number of atoms and vacancies, respectively, and d_X the X-ray density which is evaluated from the observed lattice constant (Fig. 2) and d_{obs} the observed density. As pointed out previously [12,13], the use of bulk material for obtaining d_{obs} can lead to incorrect results due to micropores generated during solidification, the existence of which always makes the apparent value small, resulting in overestimation of c_V. In order to check a reliability of estimation of c_V by the plate samples, powdered samples with a size of 60–160 μm were also prepared, similarly as used in previous work [13–15], and the density was measured for some quenching temperatures. In Co_2MnGe and Co_2MnSn, evaluated c_V values for powder samples quenched from T_Q = 773 K showed a certain decrease from those for plate samples at the same T_Q; the deviations of c_V (%) were 1.2% in Co_2MnGe and 0.3% in Co_2MnSn. Consequently, for all the c_V data by the plate samples, they were corrected by subtracting this deviation.

The plate samples (about 1 mm × 1 mm × 15 mm) for the electrical resistivity measurement were prepared for Co_2MnGe and Co_2MnSn. It was performed by a standard DC four-terminal method in a similar way as in [8]. The resistivity measurement has been frequently employed for estimating the vacancy formation and migration [e.g., 19–22]. Ordinary way to evaluate the activation energy of the vacancy migration is that change in the resistivity during ageing at lower temperatures is measured by using the samples quenched from higher temperatures. In the present study, however, we adopted the following conventional way for rough estimation of the vacancy migration for these Co_2MnGe and Co_2MnSn alloys. Namely, the samples slow-cooled from 1173 K were used for ageing experiment. Each sample was set in the furnace and first heated from room temperature to 1173 K at a rate of 5 K/min. At this temperature, it was held for 15 min. Then, after furnace-cooled down to desired temperatures of 773–873 K at averaged rate of about 50–60 K/min, the electrical resistivity was measured at intervals of 10 or 20 s, keeping the temperature constant within ±0.25 K. The measurement was made for five (Co_2MnGe) or four (Co_2MnSn) different ageing temperatures. For comparison, another ageing experiment was also performed based on the ordinary way mentioned above by using the quenched sample of Co_2MnGe; the sample was first water-quenched from 1173 K in a similar way as in the density measurement (without crushing silica tube) and then, after heated from room temperature to 773 K at a rate of about 70 K/min, the measurement was started.

Further, the other plate samples (about 5 mm × 5 mm × 1 mm) for positron annihilation measurement were prepared for Co_2MnSi, Co_2MnGe and Co_2MnSn. In a similar way as in the density measurement, after these plate samples were slow-cooled from 1173 K, they were again heated to 773 K and then water-quenched. A $^{22}NaCl$ positron source with an activity of 680 kBq sealed by kapton films with 6 μm thickness was used for the positron lifetime and coincidence Doppler broadening (CDB) measurements. This film was sandwiched between two identical samples. Positron lifetime measurement was made with the conventional fast–fast coincidence circuit with a BaF_2 scintillator with the time resolution of 190–200 ps at room temperature [23]. The CDB measurement was made by recording the energy shifts of two annihilation 511 keV photons in coincidence [24]. The spectrometer consists of two pure Ge detectors facing each other, where the sample sandwich was placed in the center. As reference samples, plate samples of pure Co, Mn, Si, Ge and Sn were also prepared for the CDB measurement. The positron lifetime and CDB spectra consisted of 1.0×10^6 and more than 10^9 counts, respectively.

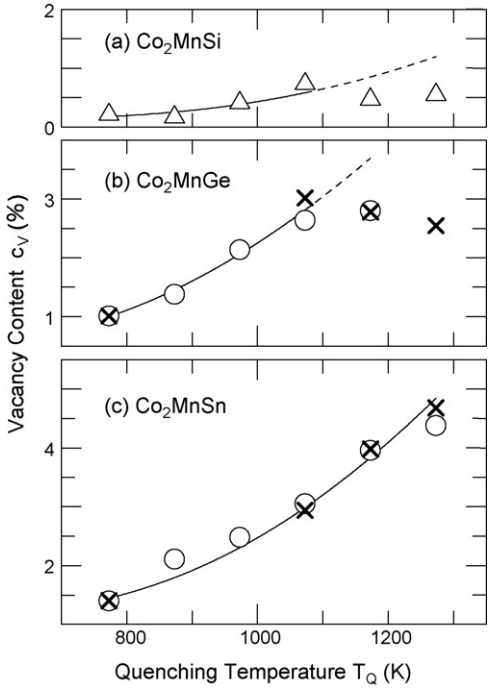

Fig. 3. Quenching temperature dependence of the vacancy concentration c_V for Co_2MnSi (a), Co_2MnGe (b) and Co_2MnSn (c) alloys. The open triangles and cross-marks represent the data by the plate samples and powder samples, respectively. The open circles represent the corrected plate sample data (see Section 2). Error bars are omitted from the figure, since the size is nearly the same as that of symbol marks used.

3. Results and discussion

3.1. Vacancy concentration

The quenching temperature dependence of the vacancy concentration c_V is shown in Fig. 3 for Co_2MnSi in (a), Co_2MnGe in (b) and Co_2MnSn in (c). The open triangles and cross-marks represent the results obtained for the plate samples and the powder samples, respectively. As mentioned in previous section, the plate sample data are corrected for Co_2MnGe and Co_2MnSn, which are plotted by the open circles (Fig. 3(b) and (c)). Agreement with corresponding powder sample data is good. The solid and dotted curves represent the fitting curves, which are mentioned in later Section 3.4.1. The vacancy concentration c_V increases with increase in quenching temperature T_Q up to 1073 K in Co_2MnSi and Co_2MnGe and up to 1273 K in Co_2MnSn. The slope is rather gradual for Co_2MnSi, while very steep for Co_2MnGe and Co_2MnSn, corresponding well to the observed trend in the lattice constant a shown in Fig. 2. Furthermore, in Co_2MnSi (Fig. 3(a)) and Co_2MnGe (Fig. 3(b)), reduction of c_V values from the dotted curves is recognized above 1073 K, which just corresponds to the inflection found in a of these alloys (Fig. 2). Therefore, it can be said that there is a certain correlation between changes in the vacancy concentration and the lattice constant in the present Heusler alloys. As to the reduction of c_V in Co_2MnGe, it is discussed in later Section 3.4.2.

3.2. Electrical resistivity

Prior to the ageing experiment, we have measured the change in electrical resistivity, ρ, with temperature, T, for Co_2MnGe and Co_2MnSn, at heating and cooling rates of 2 K/min. The results are shown in Fig. 4 by the solid curves (heating process) and dotted ones (cooling process). In both alloys, an inflection is clearly found, which will be due to a magnetic transition since the inflection points

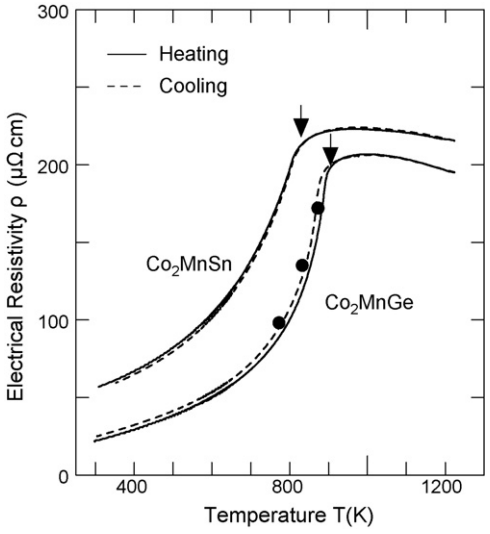

Fig. 4. Change in the electrical resistivity ρ with temperature T in Co_2MnGe and Co_2MnSn alloys. Heating and cooling rates are 2 K/min. The arrows represent the Curie temperature [25]. The dot marks represent the final resistivity ρ_f in ageing experiment (Fig. 5) for Co_2MnGe (Section 3.4.2).

are close to the Curie temperature, T_C [25], shown by the arrows. A feature to be noted is that the resistivity ρ shows a slight decrease after reaching its maximum above T_C. Such a negative temperature dependence of ρ in a range $T > T_c$ has been already reported in some $D0_3$-type ferromagnetic ternary alloys $(Fe_{1-x}M_x)_3X$ (e.g., X = Ga and Si, and M = Ti and V) [26,27].

The change in the electrical resistivity ρ with ageing at three different temperatures of 773 K (or 783 K) to 873 K is shown in Fig. 5(a)–(c) for Co_2MnGe and Fig. 6(a)–(c) for Co_2MnSn. In Fig. 5(c), the result obtained for the quenched sample is shown (similar result was also obtained for the slow-cooled sample). The resistivity ρ is found to decrease exponentially with ageing time for any ageing temperature, indicating a typical relaxation behavior. The rate constant, τ (defined in later Section 3.4.2) becomes larger with decrease in ageing temperature as found from the values given in the figures.

3.3. Positron annihilation

The results of positron lifetime for the samples quenched from 773 K were:

150 ± 2 ps for Co_2MnSi, 160 ± 2 ps for Co_2MnGe

and 175 ± 2 ps for Co_2MnSn.

These were evaluated from single component analysis. We attempted also to analyze the lifetime spectrum of these alloys based on the two-state (defect free and defect) trapping model [28], but the defect component intensity became 100% in practice, which means that all the positrons are trapped and annihilated at defect (i.e., vacancy) sites [23]. It is noted that measured lifetime value in present Co_2MnZ alloys becomes larger in the order of Z = Si, Ge and Sn, just corresponding to the order found in the lattice constant difference at T_Q = 773 K between these alloys (Fig. 2). Therefore, it can be said that the present lifetime has a similar feature as in the delocalized positron lifetime (bulk lifetime) in many metals and binary alloys, where it tends to increase with increase in free volume of vacancy, i.e., decrease in the electron density [29].

Fig. 7 shows the CDB spectrum (the thick solid curves) for Co_2MnSi in (a), Co_2MnGe in (b) and Co_2MnSn in (c), as a function of electron momentum, P_L, in m_0c-unit (m_0 the electron mass at rest and c the light velocity). In the figure, spectrum of pure Co,

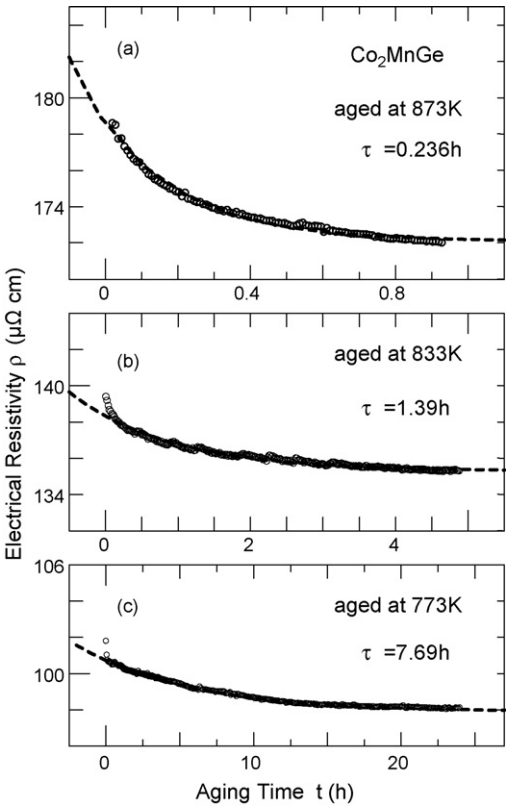

Fig. 5. Change in the electrical resistivity ρ with ageing time t in Co_2MnGe. Ageing temperatures are 873 K (a), 833 K (b) and 773 K (c). These results are for the samples slow-cooled from 1173 K, except for (c) where the quenched sample from 1173 K is used.

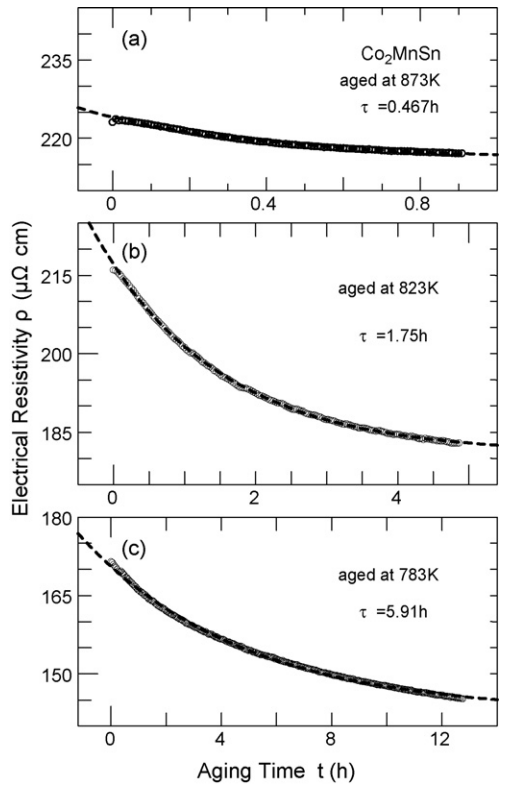

Fig. 6. Change in the electrical resistivity ρ with aging time t in Co_2MnSn. Ageing temperatures are 873 K (a), 823 K (b) and 783 K (c). These results are for the samples slow-cooled from 1173 K.

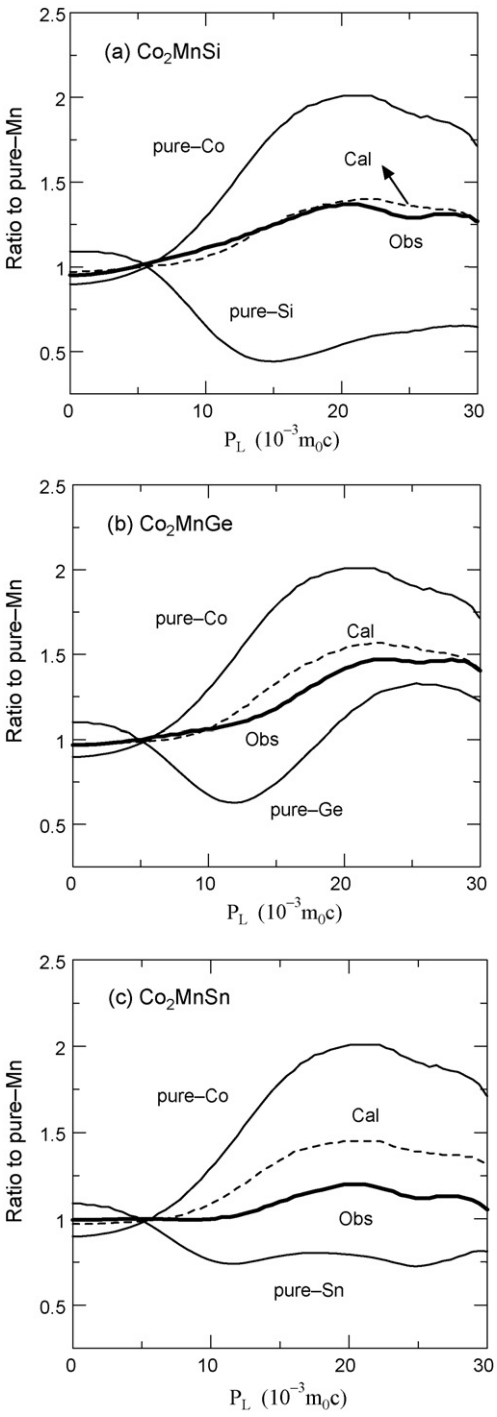

Fig. 7. Coincidence Doppler broadening (CDB) spectrum (thick solid lines) for Co_2MnSi (a), Co_2MnGe (b) and Co_2MnSn (c). These alloys were quenched from 773 K. Each spectrum is normalized to that in pure Mn. In (a)–(c), the spectra for pure Co and the corresponding pure Si, Ge or Sn are also shown (thin solid lines). The dotted curves represent the calculated spectra under the assumption of random vacancy distribution (see Section 3.4.3).

together with that of pure Si, Ge or Sn, is also given by the thin solid line. These are given in the form of the ratio of the CDB intensity to that for pure Mn. The CDB spectrum, particularly in higher momentum side (about $P_L > 10^{-2} m_0 c$), gives important information about the atomic configuration around the vacancy sites (the sites on which vacancies are located). This is because positrons trapped at the vacancy sites will be annihilated with the inner shell electrons (probably, *d*-electrons in the momentum range concerned

Table 1
Formation and migration energies of thermal vacancy, E_f and E_m, for the present Heusler ($L2_1$)-type Co_2MnZ alloys. For comparison, published experimental data for some B2-type and $D0_3$-type binary alloys are also listed. For the experimental data of other binary alloys, see [18,30,31].

Alloy (structure)	E_f (eV)	E_m (eV)	Alloy (structure)	E_f (eV)	E_m (eV)
Co_2MnSi ($L2_1$)	0.50(3)		Co_2MnGe ($L2_1$)	0.34(2)	2.0(2)
Co_2MnSn ($L2_1$)	0.40(3)	1.8(1)			
$Fe_{0.56}Al_{0.44}$ (B2)	0.83[a]	1.67[b]	FeAl (B2)	0.51(7)[c]	
CoGa (B2)	0.68[d]	1.9[d]	Fe_3Al ($D0_3$)	1.18(4)[e]	1.3(1)[e]

[a] [22].
[b] [21].
[c] [15].
[d] [18].
[e] [17].

here) of atoms adjacent to these vacancy sites. From Fig. 7, shape of the spectrum for each sample is found to resemble that for pure Co. Thus, the vacancy site seems to be the Mn-site or the Z-site or both sites, because these sites are surrounded by the Co-sites (Co atoms). However, the spectrum much more resembles the dotted curve that represents the calculated spectrum, which is discussed in later Section 3.4.3.

3.4. Discussion

3.4.1. Vacancy formation and its effective volume

As suggested previously [10], present results (Fig. 3) showed that a large amount of vacancies are formed, particularly in Co_2MnGe and Co_2MnSn alloys, where the vacancy concentration c_V reaches 2.8% at $T_Q = 1073$ K in the former and 4.4% at $T_Q = 1273$ K in the latter. Formation of a high thermal vacancy concentration, as mentioned in Section 1, has been already reported in some B2-type and $D0_3$-type binary alloys. For example, in the B2 $Fe_{1-x}Al_x$ alloy ($0.45 < x < 0.51$) case, c_V increases steeply with increase in quenching temperature, e.g., in $x = 0.509$, $c_V = 1.2\%$ at $T_Q = 773$ K and 2.8% at 1173 K [15]. Note that the present observation (Fig. 3(b) and (c)) indicates a comparable change with this. Following the previous work [15], we attempted to estimate the vacancy formation energy, E_f, for the present alloys, by assuming the following relation:

$$c_V = c_V^0 + A \exp\left(\frac{-E_f}{k_B T_Q}\right) \tag{2}$$

where c_V^0 and A are constant quantity and k_B the Boltzmann constant. In the fitting calculation, all the c_V data (Fig. 3) were used, except for those at $T_Q > 1073$ K in Co_2MnSi and Co_2MnGe. The results of E_f are listed in Table 1. In this table, the values of vacancy migration energy, E_m, described in next subsection, and for comparison, published data for some B2- and $D0_3$-type binary alloys are also listed. The solid and dotted curves in Fig. 3 represent the numerical results obtained by using Eq. (2). The calculation (solid curves) is found to reproduce well the observation. Further, it is recognized from Table 1 that the values of E_f in the present alloys are comparable with those for B2 FeAl and CoGa alloys (particularly in Co_2MnGe, it becomes rather small) and are quite smaller than for $D0_3$ Fe_3Al alloy, indicating ease of thermal vacancy creation. As pointed out by Schaefer and Bedula-Gergen [18], the formation energy is thought to relate to the structure. For examples, $L1_2$-type and $L1_0$-type structures belong to a group of fcc-based (closely packed) structure. In binary alloys with these structures, their formation energy E_f tends to have much larger value than for the binary alloys with bcc-based (loosely packed) structures; e.g., 1.82 eV for $L1_2$ Ni_3Al alloy and 1.4 eV for $L1_0$ TiAl alloy [18]. As mentioned in Section 1, Heusler-type structure is the bcc-based structure and so, such lower formation energy in the present alloys may be acceptable.

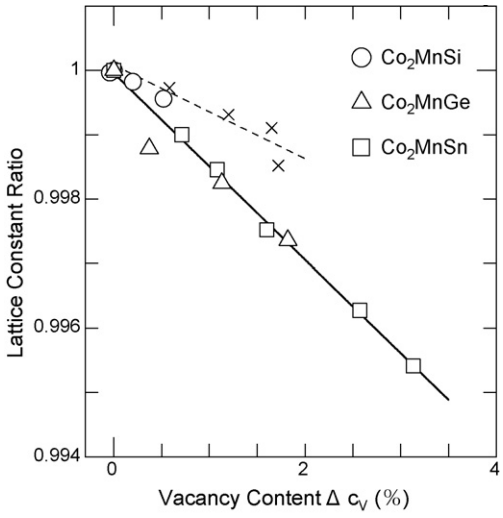

Fig. 8. Relation between the lattice constant ratio a/a_0 and the vacancy concentration difference Δc_V in Co_2MnSi (circles), Co_2MnGe (triangles) and Co_2MnSn (squares). For comparison, the data for B2-type FeAl alloy [15] are also shown by the cross-marks.

We next discuss a relation between the lattice constant a (Fig. 2) and the vacancy concentration c_V (Fig. 3). This is shown in Fig. 8 for Co_2MnSi (circles), Co_2MnGe (triangles) and Co_2MnSn (squares), where a is normalized to a_0 (the value at $T_Q = 773$ K) and plotted as a function of Δc_V (the difference in c_V from that at $T_Q = 773$ K). The data of $T_Q > 1073$ K in Co_2MnSi and Co_2MnGe are omitted from the figure. A linear relation is clearly found between these. As noted in previous work on B2 $Fe_{1-x}Al_x$ alloys [15], the reduction of the lattice constant may be understood as volume relaxation in unit cell due to retained vacancies. Then, the change in a will be interpreted in terms of atomic size effect and it is expressed as [15]

$$a = (16)^{1/3}\left\{(1-c_V)\Omega_A + c_V\Omega_V\right\}^{1/3} \approx \left(16\Omega_A\right)^{1/3}\left\{1 - \frac{1}{3}\frac{\Omega_A - \Omega_V}{\Omega_A}c_V\right\} \tag{3}$$

where Ω_A represents the averaged atomic volume of Co_2MnZ alloy in vacancy free state and Ω_V represents the effective vacancy volume. From Eq. (3), the ratio a/a_0 can be approximated by a linear form with respect to Δc_V as follows:

$$\frac{a}{a_0} = 1 - \frac{1}{3}\frac{\Omega_A - \Omega_V}{\Omega_A}\Delta c_V \tag{4}$$

Since effective vacancy volume Ω_V is smaller than Ω_A, the ratio a/a_0 is found to decrease linearly with increase in Δc_V. The volume ratio Ω_V/Ω_A can be evaluated from Eq. (4) by using the data shown in Fig. 8. The solid line in Fig. 8 indicates the numerical result for $\Omega_V = 0.565\Omega_A$. It is noted that almost all the data points are located on this line, independent of alloy. For comparison, the result for B2 FeAl alloy [15] is shown by the cross-marks and the dotted line represents the numerical result for $\Omega_V = 0.782\Omega_A$. The slope is found to be steeper in the present Heusler alloys than in B2 FeAl alloy, which means that a degree of volume relaxation due to vacancy formation is larger in the present alloys. The volume ratio Ω_V/Ω_A that gives a measure of volume relaxation will depend on alloy, e.g., its strength of atomic bonding and its crystal structure, and further, on vacancy type and vacancy site (described in later Section 3.4.3). So, the features pointed out above will be understood by examining carefully the relation to these factors. Further experimental and theoretical studies are needed.

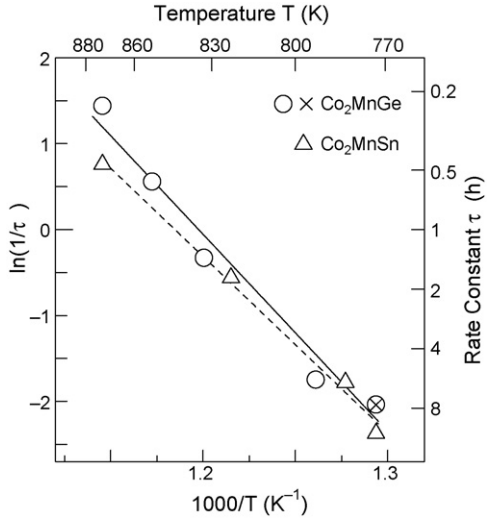

Fig. 9. Arrhenius plot of the reciprocal rate constant τ and temperature T in Co_2MnGe (circles) and Co_2MnSn (triangles) alloys (cf. Figs. 5 and 6). The cross-mark at $T = T_A = 773$ K represents the result of Co_2MnGe (quenched sample).

3.4.2. Vacancy migration

Present observation of the electrical resistivity ρ certainly indicated a relaxation behavior during ageing (Figs. 5 and 6). For comparison, we performed a similar ageing experiment at 873 K using pure Fe with high vacancy formation energy of 1.6 eV [32]. As a result, any appreciable change in ρ could not be detected (it was kept constant within ±0.07%), which may be due to very small vacancy content (about 1 ppm order at 1173 K). On the other hand, the reduction of ρ during ageing reaches about 2–4% in Co_2MnGe and 4–20% in Co_2MnSn. Therefore, the observed relaxation behavior is interpreted as annealing process toward equilibrium, in which the retained excess vacancies by furnace-cooling from 1173 K will be annealed-out during ageing through the vacancy migration. This behavior may be well expressed as [17,19,20]

$$\rho(t) = \rho_f + \left(\rho_i - \rho_f\right) \exp\left(\frac{-t}{\tau}\right) \tag{5}$$

where $\rho(t)$ the resistivity ρ at ageing time t, ρ_I and ρ_f the initial and final values of ρ and τ the rate constant. Numerical results are shown by the dotted curves in Figs. 5(a)–(c) and 6(a)–(c). Respective curve is found to reproduce well the observation. Evaluated values of rate constant τ are also given in the figures. The final resistivity ρ_f (Eq. (5)) may give the equilibrium value at respective ageing temperature. We can compare ρ_f with the corresponding value of ρ in Fig. 4 (cooling process) which shows the temperature dependence of ρ. Dot marks in Fig. 4 represent the values of ρ_f in the Co_2MnGe case. Their difference is found to be not so large (less than 6%). However, in the Co_2MnSn case (Fig. 6(b) and (c)), it becomes rather large (about 13–20%). The reason of this large difference is not clear.

For rough estimation of the vacancy migration energy E_m, for Co_2MnGe and Co_2MnSn alloys, we adopted the following relation [17,19,20,33]:

$$\tau^{-1} = C \exp\left(\frac{-E_m}{k_B T_A}\right) \tag{6}$$

where C is a constant quantity and T_A represents the ageing temperature. $\ln(1/\tau)$ vs. $1/T$ plot is shown in Fig. 9 for Co_2MnGe (circles) and Co_2MnSn (triangles). The cross-mark at $T = T_A = 773$ K represents the result obtained from the quenched sample of Co_2MnGe (Fig. 5(c)), which agrees well with corresponding result by the slow-cooled sample. The solid and dotted lines represent the numerical results for Co_2MnGe and Co_2MnSn, respectively. The migration energy E_m for these alloys can be evaluated from the slope of respective line. The results are listed in Table 1. A comparatively large error size may come from small number of data and some scattering of data points. Taking into account this size, distinct difference in E_m is not recognized between these alloys. Further, their values are found to be comparable with those for B2 $Fe_{0.56}Al_{0.44}$ and CoGa alloys.

As mentioned in Section 3.1, observed vacancy concentration c_V in Co_2MnSi and Co_2MnGe showed a deviation from the theoretical curve given by Eq. (2) at high quenching temperatures of $T_Q > 1073$ K (Fig. 3(a) and (b)). Similar behavior was also observed in B2 $Fe_{1-x}Al_x$ alloys [15]. In general, the mobility of vacancies that will lead to elimination of vacancies during quenching is enhanced as the temperature becomes higher [15]. In order to retain the vacancy concentration at high temperatures, rapid quenching that overcomes the vacancy mobility will be needed. So, when the quenching rate is not so high as to prevent the elimination of vacancies, retained vacancy concentration will be lowered from the expected value (Eq. (2)), as observed in Co_2MnSi and Co_2MnGe alloys. On the other hand, in Co_2MnSn, such a deviation is not detected until $T_Q = 1273$ K (Fig. 3(c)) despite employing the same quenching method. This suggests that vacancy mobility in Co_2MnSn is lower than that in other two alloys at higher temperatures. For rough examination of this suggestion, we evaluated the rate constant τ for Co_2MnGe and Co_2MnSn at high temperatures T, since the vacancy mobility will relate to the rate constant τ (i.e., higher mobility results in a shorter rate constant). From Eq. (6), the ratio τ/τ_0 (τ_0 the rate constant at reference temperature T_0) is given in terms of T, T_0 and E_m, and thus, it can be obtained when using the observed values of E_m (Table 1). Taking the reference temperature as $T_0 = 873$ K (for τ_0, cf. Figs. 5(a) and 6(a)), the evaluated values of τ were 6.4 s at $T = 1073$ K, 1.0 s at 1173 K and 0.2 s at 1273 K for Co_2MnGe, while 21 s (1073 K), 4.1 s (1173 K) and 1.0 s (1273 K) for Co_2MnSn, indicating a much longer rate constant in Co_2MnSn (e.g., at $T = 1173$ K, it becomes four times longer than in Co_2MnGe). Consequently, we can expect that the vacancy mobility becomes higher for Co_2MnGe in high-temperature region concerned and so, this will result in reduction of the vacancy concentration in this alloy, shown in Fig. 3(b).

Furthermore, such higher mobility in Co_2MnGe may affect also the electrical resistivity behavior due to ageing (Fig. 5), particularly for the initial resistivity ρ_i (Eq. (5)). Namely, when the sample is furnace-cooled from 1173 K, more excess vacancies will be annealed-out so that the retained vacancy concentration in the initial stage of ageing (corresponding to ρ_i) will be rather close to the final (or equilibrium) concentration at this ageing temperature (corresponding to the final resistivity ρ_f). Comparatively small difference between ρ_i and ρ_f in Co_2MnGe (Fig. 5(b) and (c)), compared with that in Co_2MnSn (Fig. 6(b) and (c)), may come from this situation.

3.4.3. Vacancy type and vacancy site

As mentioned in Section 3.3, present measured positron lifetime (150 ps for Co_2MnSi, 160 ps for Co_2MnGe and 175 ps for Co_2MnSn) indicates the lifetime coming from annihilation of positrons trapped at the vacancy sites. We first consider the vacancy type appearing in the present Co_2MnZ alloys, based on the positron annihilation studies for many metals and binary alloys [e.g., 17,18,23,24,29,30,32,34], where mainly the mono-vacancy and sometimes the di-vacancy were investigated. Examples of the lifetime values are 175 ps for pure Fe and 160 ps for pure Ni [29] in the metal case, and, about 180 ps for B2 $Fe_{1-x}Al_x$ ($x \leq 0.41$) [30], 173 ps for $D0_3$ Fe_3Al [30], 184 ps for B2 NiAl [29] and 181 ps for $L1_2$ Ni_3Al [29] in the binary alloy case, which are thought to be for the mono-vacancy. Present result is comparable with these data and thus, we can suppose that the vacancies formed in the present alloys are mono-vacancies. In B2 $Fe_{1-x}Al_x$ alloys, however, other than the mono-vacancy located on the Fe-site (V_{Fe}), formation of

di-vacancy was also reported in higher Al concentration ($x \geq 0.42$) and higher temperature (above 1000 K) ranges where the vacancy concentration becomes higher [23,24,30,34]. In the $Fe_{0.52}Al_{0.48}$ alloy case, the lifetime value increased from 185 ps below about 1000 K to 194 ps above about 1200 K [30]. This was interpreted as the change in the kind of di-vacancy, i.e., from two vacancies located on the second nearest neighboring Fe-sites ($2V_{Fe}$) to those on the nearest neighboring Fe- and Al-sites ($V_{Fe}V_{Al}$) [30]. Note that the present result is only for quenching temperature of T_Q = 773 K. Since the vacancy concentration becomes higher by further increase in T_Q (Fig. 3), there is a possibility of formation of such di-vacancies at high temperatures.

Next, we examine on which site the vacancies are located. In Heusler Co_2MnZ alloys, there are three kinds of mono-vacancy; Co-vacancy V_{Co} (vacancy on the Co-site), Mn-vacancy V_{Mn} and Z-vacancy V_Z. As mentioned in previous Section 3.3, the shape of the CDB spectrum for each alloy resembles the spectrum for pure Co (Fig. 7). This suggests a formation of mono-vacancies V_{Mn} or V_Z or both, because the positrons trapped at vacancy sites will be annihilated with electrons of neighboring Co atoms. However, the sample spectrum itself is rather far away from the Co spectrum in the important region, indicating an existence of Co-vacancy V_{Co} in addition to above two. For simplicity, we here consider only the case in which all the vacancies are randomly distributed over the sites. Then, the fractions of mono-vacancies V_{Co}, V_{Mn} and V_Z are given by 0.5, 0.25 and 0.25, respectively, so that expected sample spectrum may be given as the summation of the Co, Mn and Z spectra multiplied by the respective fractions. Calculated spectra are shown by the dotted curves in Fig. 7. Agreement with the observation is found to be improved, particularly in Co_2MnSi (Fig. 7(a)) and Co_2MnGe (Fig. 7(b)). In the Co_2MnSn case (Fig. 7(c)), it is not still so good and thus, this alloy may contain the Co-vacancies more than $N_V/2$.

In the previous study [10], a distinct correlation between the atomic disorder (antisite atoms) and the magnetism was found in the present Heusler alloys. The formation of large amount of thermal vacancies, which was confirmed by the present study, is thought to affect various properties of these alloys. However, a distinct relation between the vacancy formation and the magnetism is not recognized. If the state of random vacancy distribution mentioned above is unchanged even at higher temperatures and this state affects hardly their magnetism, such situation may be acceptable. Even in this case, however, the reason must be clarified. For understanding the role of vacancies, much more detailed study on the vacancy behaviors is needed from experimental as well as theoretical approaches.

4. Conclusion

Thermal vacancy formation was studied for the Heusler-type ferromagnetic alloys Co_2MnSi, Co_2MnGe and Co_2MnSn as a function of temperature (quenching temperature). Concluding remarks are as follows:

(1) The vacancy concentration determined from the density and lattice constant [10] measurements increased with increase in quenching temperature up to 1073 K or 1273 K. Particularly in Co_2MnGe and Co_2MnSn, a high vacancy concentration exceeding 2% was observed at high quenching temperatures. Further, a distinct linear relation was found between the vacancy concentration and the lattice constant.
(2) Change in the electrical resistivity due to ageing at various temperatures of 773–873 K showed a relaxation behavior in Co_2MnGe and Co_2MnSn. This is due to annealing-out of the excess vacancies retained during furnace-cooling from 1173 K.
(3) The vacancy formation and migration energies were evaluated from the above measurements. These values are comparable with those for B2-type FeAl and CoGa alloys generating a high concentration of thermal vacancies.
(4) The vacancy type and the vacancy site were examined for the quenched alloys from 773 K by the positron lifetime and coincidence Doppler broadening measurements. As a result, it was suggested that the mono-vacancies are randomly distributed over the lattice sites.

Acknowledgements

The authors wish to thank Professor T. Takasugi, Dr. Y. Kaneno and Dr Y. Kubota of Osaka Prefecture University for kind help in sample preparation, Dr H. Ishibashi of Osaka Prefecture University for valuable suggestions and Mr. T. Akagawa (present address: Dai Nippon Printing Co. Ltd, Tokyo, 162-8472, Japan) for devoted help in the density measurements.

References

[1] S. Fujii, S. Sugimura, S. Ishida, A. Asano, J. Phys. Condens. Matter. 2 (1990) 8583.
[2] I. Galanakis, P.H. Dederichs, N. Papanikolaou, Phys. Rev. B66 (2002) 174429.
[3] I. Galanakis, P.H. Mavropoulas, P.H. Dederichs, J. Phys. D: Appl. Phys. 39 (2006) 765.
[4] Y. Miura, K. Nagao, M. Shirai, Phys. Rev. B69 (2004) 144413.
[5] S. Picozzi, A. Continenza, A.J. Freeman, Phys. Rev. B69 (2004) 094423.
[6] Y. Miura, M. Shirai, K. Nagao, J. Appl. Phys. 99 (2006) 08J112.
[7] I. Galanakis, K. Ozdogan, B. Aktas, E. Sasioglu, Appl. Phys. Lett. 89 (2006) 042502.
[8] M. Kogachi, N. Tadachi, T. Nakanishi, Intermetallics 14 (2006) 742.
[9] T. Fujiwara, S. Kikuchi, H. Ishibashi, M. Kogachi, Mater. Res. Soc. Symp. Proc. 980 (2007) II05–15.
[10] M. Kogachi, T. Fujiwara, S. Kikuchi, J. Alloys Compd., in press.
[11] M. Kogachi, N. Tadachi, H. Kohata, H. Ishibashi, Intermetallics 13 (2005) 535.
[12] A.H. van Ommen, A.A.H.J. Waegemaekers, A.C. Moleman, H. Schlatter, H. Bakker, Acta Metall. 29 (1981) 123.
[13] M. Kogachi, T. Tanahashi, Y. Shirai, M. Yamaguchi, Scr. Mater. 34 (1996) 243.
[14] M. Kogachi, T. Tanahashi, Scr. Mater. 35 (1996) 849.
[15] M. Kogachi, T. Haraguchi, Mater. Sci. Eng. A 230 (1997) 124.
[16] K. Harada, H. Ishibashi, M. Kogachi, Mater. Res. Soc. Symp. Proc. 753 (2003), BB5.28.1.
[17] R. Wurschum, C. Grupp, H.E. Schaefer, Phys. Rev. Lett. 75 (1995) 97.
[18] H.E. Schaefer, K. Bedula-Gergen, Defect Diff. Forum 143–147 (1997) 193.
[19] M.S. Wechsler, Acta Metall. 5 (1957) 150.
[20] J.P. Rivier, J. Grilhe, Acta Metall. 20 (1972) 1275.
[21] J.P. Rivier, J. Grilhe, Phys. Stat. Solidi. (a) 25 (1974) 429.
[22] J.P. Rivier, J. Grilhe, Scr. Metall. 9 (1975) 967.
[23] T. Haraguchi, F. Hori, R. Oshima, M. Kogachi, Intermetallics 9 (2001) 763.
[24] B. Somieski, J.H. Schneibel, L. Hulett, Philos. Mag. Lett. 79 (1999) 115.
[25] P.J. Webster, J. Phys. Chem. Solids 32 (1971) 1221.
[26] N. Kawamiya, Y. Nishiono, M. Matsuo, S. Asano, Phys. Rev. B44 (1991) 12406.
[27] Y. Nishiono, S. Inoue, S. Asano, N. Kawamiya, Phys. Rev. B48 (1993) 13607.
[28] A. Vehanen, P. Hautojarvi, J. Johanson, J. Yli-Kauppila, Phys. Rev. B25 (1982) 762.
[29] R. Wurschum, K. Badula-Gergen, E.A. Kummerle, C. Grupp, H.E. Schaefer, Phys. Rev. B54 (1996) 849.
[30] A. Broska, J. Wolff, M. Franz, Th. Hehenkamp, Intermetallics 7 (1999) 259.
[31] M. Kogachi, High Temp. Mater. Process. 18 (1999) 269.
[32] H.E. Schaefer, Proceedings of the International Conference on Positron Annihilation, 1985, p. 448.
[33] M. Kogachi, H. Ishibashi, T. Ohba, X. Ren, K. Otsuka, Scr. Mater. 42 (2000) 841.
[34] J. Wolff, M. Franz, A. Broska, B. Kohler, Th. Hehenkamp, Mater. Sci. Eng. A239–240 (1997) 213.